Traces of cathode glow in atmospheric surface dielectric barrier discharge

S. Y. Kim, T. Lho, and K.-S. Chung

Citation: AIP Advances **8**, 125321 (2018); doi: 10.1063/1.5054910
View online: https://doi.org/10.1063/1.5054910
View Table of Contents: http://aip.scitation.org/toc/adv/8/12
Published by the American Institute of Physics

Traces of cathode glow in atmospheric surface dielectric barrier discharge

S. Y. Kim,[1,a] T. Lho,[2] and K.-S. Chung[1]
[1]*Department of Electrical Engineering, Hanyang University, Seoul 04763, South Korea*
[2]*Plasma Technology Research Center of National Fusion Research Institute (NFRI), Gunsan, Jeonbuk 54006, Korea*

(Received 4 September 2018; accepted 6 December 2018; published online 17 December 2018)

Owing to the cathode layer properties in atmospheric surface dielectric barrier discharges (SDBDs), the discharges are sustained both for positive and negative voltage phase. There should be the cathode glow region where excited molecules or atoms are produced due to collision with the electrons before occurrence of electron-ion breeding in the cathode layer. Although a previous numerical study reported the generation of oxygen atoms, $O(^1D)$, $O(^3P)$, near an exposed electrode (EE) during the negative voltage phase, it is experimentally unattainable to verify the existence of the oxygen atoms because of the short length of the cathode layer with a thickness of approximately 20 μm at 1 atm in filamentary discharge mode. This work presents the experimental confirmation of trace(s) of O and N, which indicates the cathode glow, in a cathode layer in atmospheric SDBDs using ultra-fine surface polyimide as a dielectric in SDBD. Our results show that the cathode glow in atmospheric SDBD is located at approximately 5~6 μm from EE in air. https://doi.org/10.1063/1.5054910

I. INTRODUCTION

A cathode glow is the region where excited atoms and molecules collide with energetic electrons to emit light before electron-impact ionization.[1] Previous articles have reported the cathode layer parameters[2–4] of atmospheric surface dielectric barrier discharge (SDBD) by numerical simulation. Anohkin et al.[5] reported the production of oxygen atoms such as $O(^1D)$, $O(^3P)$, and $O(^1S)$[5,6] near an exposed electrode by the electron-impact dissociation of oxygen molecules, which could be evidence of cathode glow in atmospheric SDBD. Reactive nitrogen species (RNS) such NO_2, N_2O_5, and N_2O measured in atmospheric SDBD using Fourier Transform Infrared Ray (FT-IR) spectroscopy[7] are generated through the complex reaction paths involving nitrogen atoms in air plasmas.[8]

However, the experimental observation of the excited species near an exposed electrode of SDBD at high pressure with current optical technologies[9,10] is unattainable because the cathode layer thickness is inversely proportional to the gas pressure.[11] Moreover, the short life-time of the excited atoms such as $O(^1D)$ and N renders the observation more difficult in air filamentary discharges.[12]

The experimental visualization of the cathode layer in atmospheric SDBD was reported by using polyimide with ultra-fine surface roughness as a dielectric in SDBD;[13,14] further, it was experimentally confirmed that the cathode layer thickness of atmospheric SDBD is approximately 20 μm, which has been proposed by Ref. 3 In the report the visualization of two erosion stripes on the polyimide near the exposed electrodes was clearly visible.[13] One erosion line adjacent to the exposed electrode is obviously caused by the influence of the positive ions during the negative voltage phase.[3] Although Babaeva reports the existence of the positive ions up to several tens of eV in very high *E/N*,[15] the proposed visualization method using reaction of polyimide with reactive species does not give information on the energy of positive ions reacting polyimide surface.

[a]Corresponding author: Tel : +82 2 2220 0465; fax: +82 2 2220 1894 E-mail address: hysleeper@hanyang.ac.kr

In this work, the second erosion strip was experimentally investigated by comparing the intensity of the etching lines in two SDBDs with different heights of the exposed electrodes. The difference of the exposed electrodes causes difference of brightness in glow discharge, which implies different amount of secondary electron emission ejected from the exposed electrodes.[16]

II. EXPERIMENTS

The structures of the employed SDBDs are shown in Figures 1. The heights of the exposed electrodes of the SDBDs were 8.6 μm, and 0.08 μm to obtain sufficient difference of secondary electron emission ejected from the exposed electrodes.[16] The SDBD with the exposed electrode's height of 0.08 μm shown in Figure 1 (a) was prepared by the following sequential processes: First, the polyimide surface (Kapton EN150-A, TorayDupont, Japan) was plasma-treated with DC O_2/Ar mixture at 50 mTorr. Subsequently, sequential DC magnetron sputtering of NiCr and Cu was applied at 1.5 mTorr in Ar atmosphere. Finally, wet etching using Fe_2Cl_3 performed to form a stripe of exposed electrode on one side of the copper layers on the polyimide. The two plasma processes were performed using a roll to roll sputter machine of KCFT, Korea. The SDBD with the exposed electrode's height of 8.6 μm was prepared by additional electroplating process on a thin copper layer with a thickness of 0.08 μm.

For clarifying the narrow erosion stripe in a micro spatial resolution and avoiding electric field disturbance by high roughness surface,[4] Kapton EN150-A with ultra-fine surface below 0.1 μm was used as a dielectric in SDBD shown in Figure 2 (a). Figures 2 (a)–(c) present the electron microscopy images of three SDBDs made of three different FCCLs (flexible copper clad laminates), sputtered FCCL, casting FCCL, and laminating FCCL.[17–19] The dielectric surface of the sputtered FCCL shown in Figure 2 (a) look clearly fine. However, the surfaces of the others' dielectric look very rough owing to usage of nodule-treated copper foils, which cannot give a good spatial resolution of etched surface by the reactive species.[5,13,18]

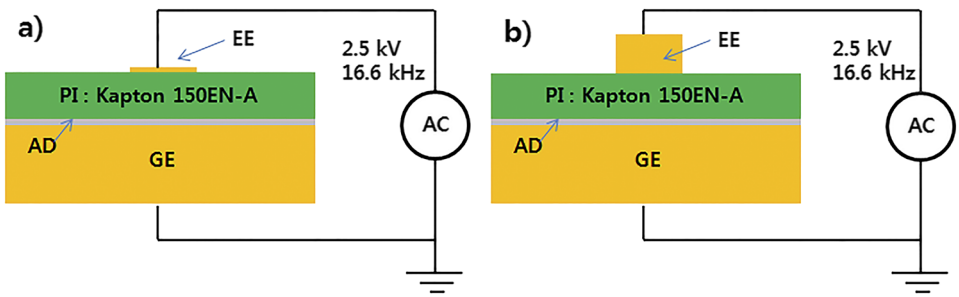

FIG. 1. Schematic views of the experiment: EE: exposed electrode (orange); PI: polyimide (dark green); AD: adhesive layer (gray); GE: ground electrode (orange); AC: high-voltage AC; heights of EE are 0.08 μm in a) and 8.6 μm in b).

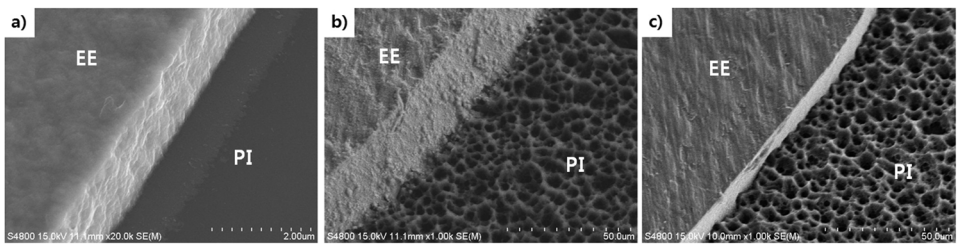

FIG. 2. Electron microscopy images of three SDBDs made of three different FCCLs with different thickness of copper layers, (a) Sputtered FCCL with a copper layer's thickness of 2 μm, (b) Casting FCCL with a copper layer's thickness of 25 μm, and (c) Laminating FCCL with a copper layer's thickness of 12 μm, EE: exposed electrode, PI: polyimide.

The high voltage AC is generated using a neon transformer (NT Electronics, Korea) and is controlled by a slidac. The applied voltage and the driven frequency are 5 kVpp and 16.6 kHz, respectively. Using a field emission secondary electron microscope (FE-SEM, S-4800, Hitachi, Japan), morphology analysis of the surface of pristine and etched SDBDs was performed.

III. RESULTS

Thin SDBDs with an exposed electrode' height of 0.08 μm were operated at different times, i.e., 20 s, 40 s, 1 min, 2 min, and 3 min. Figure 3 (a) is a 500 x magnification electron microscopy image of the pristine surface. As the discharge time increased, the etched surfaces of polyimide were remarkably observed. The width of the non-etched polyimide surface adjacent to the exposed electrode decreased with the increase in discharge time. A strip on the non-etched surface located at approximately 5~6 μm from the exposed electrode was observed, as shown in Figure 3 (c), and it is located parallel to the exposed electrode. As the discharge time increased, the stripes became vividly visible, but their location appears unchanged as shown in Figures 3 (e)(f). Owing to the undercutting by oxygen atoms at 1 atm[20] and the curled up edges of the electrodes, the location of the erosion stripes appears to be changed.

To clarify that the weak stripes are caused by the erosion phenomena resulting from the reactive oxygen species, the SDBD operated for 2 min was investigated at a 45° tilt and compared with the SDBD operated for 2 min of 8.6-μm-high exposed electrode. In Figure 4 (a) the second stripe (yellow arrow) is much more clearly visible, which indicates the local erosion of the polyimide. Compared with the second stripe in Figure 4 (b), it appears less intense. However, the width of the first stripe (green arrow) in Figure 4 (a) appears wider. Because the density of the oxygen and nitrogen atoms produced by electron-impact dissociation near a metallic exposed electrode is proportional to the number of secondary electrons ejected from the electrode,[16] we conclude that the second erosion stripes in Figures 4 (a)(b) were caused by a local surface reaction of the electrically neutral reactive oxygen and nitrogen atoms with the polyimide surface.[21]

Figures 5 (a)(b) show the electron microscopy images of the surface of SDBDs with 8.6-μm-high exposed electrode operated for 2 min. Two etching stripes are clearly visible. The second erosion stripes (yellow arrows) are also observed at approximately 5.7 μm from the exposed electrode. Interestingly, the second stripe is located almost parallel to the exposed electrode. This confirms that the erosions were caused by the reactive species strongly involved with the secondary electrons ejected from the exposed electrode.

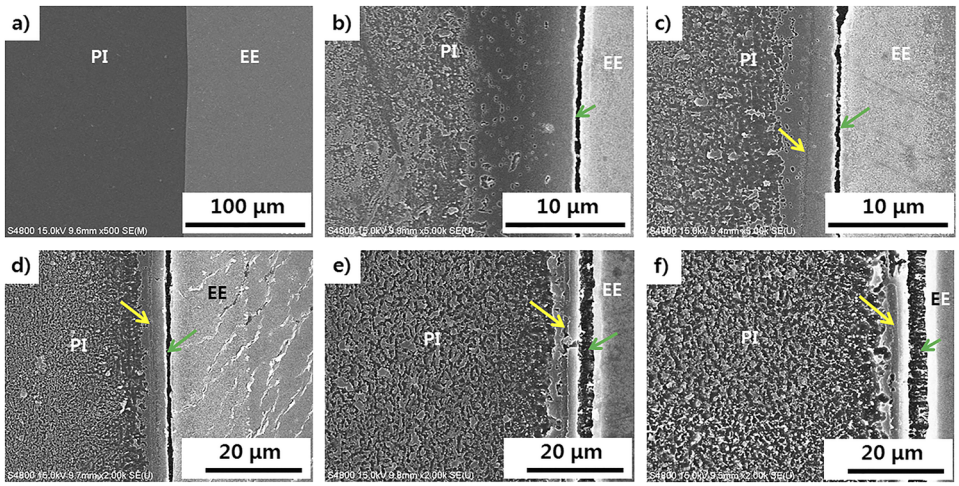

FIG. 3. Top views of the electron microscopy images of dielectric surface erosion with the time duration (T_D) of discharge. (a) T_D=0, (b) T_D=20 s, (c) T_D=40 s, (d) T_D=1 min. (e) T_D=2 min, (f) T_D=3 min. Green arrows refer to the polyimide erosion line near EE. Yellow arrows refer to the erosion line on the polyimide.

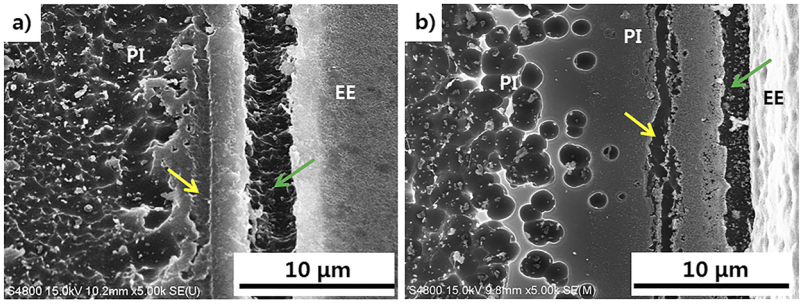

FIG. 4. a) Top view of FIG. 2 (e) obtained at a 45° tilt, and b) Top view of discharged SDBD of 8.6-μm-high exposed electrode.

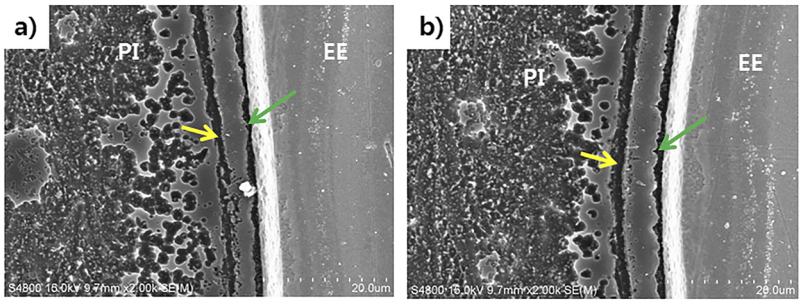

FIG. 5. Top views of discharged SDBD of 8.6 μm high exposed electrode.

IV. DISCUSSION

At 6.0 eV and 8.4 eV, O(^{3}P) and O(^{1}D) associated with the Herzberg and Schumann-Runge systems of O_2 are produced by electron-impact dissociation processes.[12] The dissociation rate coefficient significantly increases with the reduced electric field (*E/N*).[5,9,12] In atmospheric SDBD the *E/N* is the strongest near an exposed electrode,[3–5] and the dense generation of oxygen atoms near an exposed electrode during the negative nanosecond pulse was computationally simulated.[5] The case of nitrogen atoms produced by electron-impact is same with that of oxygen atoms.[8,22]

During breakdown positive ions produced by electron-impact ionization in a cathode region drift to an exposed electrode.[2–4] Then, the secondary electrons are ejected by the bombardment of the positive ions to the exposed electrode. Because drifting positive ions to the exposed electrode occurs just above dielectric surface in a cathode layer as the surface positive charges, both excitation, dissociation, and ionization by the accelerated secondary electrons also occur just above the dielectric surface.[3] An amount of secondary electrons is larger than that of initial electrons of breakdown. This indicates the second stripes in Fig. 3–5 are mostly caused by the electrically neutral oxygen and nitrogen atoms produced by the secondary electron-impact dissociation.

Both O(^{3}P) and O(^{1}D) are produced by electron-impact dissociation of O_2 in two processes with threshold energies of 6.0 and 8.4 eV.[5,10] In the reactions the amount of the O(^{3}P) is much more than that of O(^{1}D).[10] In addition, the life time (a few tens μs) of O(^{3}P) is much longer than that (10 ns) of O(^{1}D).[10] If the reactions occurred at 1 μm height over the polyimide surface, the width of etched polyimide surface by O(^{3}P) should be wider than 1 μm. However, our work shows the existence of the non-etched polyimide surface around the narrow second erosion lines., which indicates that the production of oxygen and nitrogen atoms by the electron impact occurs just above the polyimide surface located at approximately 5~6 μm from EE.

There are various active oxygen and nitrogen species, like positive and negative ions in a cathode layer in a SDBD, which etch a polyimide dielectric. However, unless particles reside or protrusions exist on the surface,[15] during the negative voltage phase positive ions etch only the adjacent of the dielectric to the exposed electrode. Negative oxygen ions (O_2^-, and O_3^-) occurred in a cathode layer become the trust forces implying no contribution to etch the surface.[3] During the positive

voltage phase the cathode layer region is filled by positive ions. However, they are repelled into a space. The reactive oxygen and nitrogen species are generated in streamer heads approaching the exposed electrode. The distance of a positive streamer head from the dielectric surface is about 30 μm according to Ref. [23], and the diffusion time scale (a few ms) of the species to the dielectric is too long considering 16.6 kHz.[3,12,23] These indicate that only reactive oxygen and nitrogen species produced in a cathode layer in AC SDBD spatially selectively react with a dielectric surface in the cathode layer at discharge frequency above a few kHz.[3,4,12,13]

With morphology analysis and selective reaction of active oxygen and nitrogen species in a cathode layer in AC SDBD, we conclude that most of the second stripes are the result of the etched polyimide surface by oxygen and nitrogen atoms produced by the secondary-electron impact during the negative polarity voltage. Because $O(^1D)$ and $O(^1S)$ are produced with $O(^3P)$, the observed second erosion line in the cathode layer presents a trace of cathode glow in atmospheric SDBD.

V. CONCLUSION

This work firstly presents the trace of cathode glow in atmospheric SDBD by using specific nature of spatiotemporally selective reactions of ionic and reactive oxygen and nitrogen species with a polyimide surface in a cathode layer. It is experimentally visualized that that the cathode glow in a cathode layer is located at approximately 5-6 μm from the exposed electrode at 1 atm in air.

ACKNOWLEDGMENTS

The support of KCFT, Korea is gratefully acknowledged for the use of instruments and material. This work was partially supported by the R&D Program (2018K000283) for Technology Upgrade through R&D Performance Management System funded by the Ministry of Science and ICT of Korea. This work is also partially supported by the National R&D Program through the National Research Foundation of Korea funded by the Ministry of Science, ICT and Future Planning (2017R1D1A1B03033076).

[1] M. A. Liberman and A. J. Lightenberg, *Principles of Plasma Discharges and Materials Processing* (Wiley-Interscience, 2005).
[2] V. I. Gibalov and G. J. Pietsch, Plasma Sources Sci. Technol. **21**, 024010 (2012).
[3] V. R. Soloviev, J. Phys D: Appl. Phys. **45**, 025205 (2012).
[4] V. R. Soloviev, I. V. Selivonin, and I. A. Moralev, Phys. Plasmas **24**, 103528 (2017).
[5] E. M. Anokhin, D. N. Kuzmenko, S. V. Kindysheva, V. R. Soloviev, and N. L. Aleksandrov, Plasma Sources Sci. Technol. **24**, 045014 (2015).
[6] J. L. Walsh and M. G. Kong, Appl. Phys. Letts. **99**, 081501 (2011).
[7] M. A. Ch. Hänsch, J. Winter, R. Bussiahn, K.-D. Weltmann, and T. von Woedtke, Plasma Medicine **3**, 27 (2013).
[8] M. Figus, Master's Thesis, Stevens Institute of Technology, QC718.5.S6 F54 (2004).
[9] Yu. P. Raizer, *Gas Discharge Physics* (Springer, Berlin, 1991).
[10] X. Zhao, S. Xu, and J. Ouyang, J Europhys. Lett. **103**, 55001 (2013).
[11] R. Wild, T. Gerling, R. Bussiahn, K.-D. Weltmann, and L. Stollenwerk, J. Phys D: Appl. Phys. **47**, 042001 (2014).
[12] B. Eliasson, M. Hirth, and U. Kogelschatz, J. Phys D: Appl. Phys. **20**, 1421 (1987).
[13] S.-Y. Kim, T. Lho, and K.-S. Chung, Phys. Plasmas **25**, 064503 (2018).
[14] R. Seeböck, H. Esrom, M. Charbonnier, M. Romand, and U. Kogelschatz, Surf. Coat. Technol. **142-144**, 455 (2001).
[15] N. Yu. Babaeva and M. J. Kushner, Plasma Sources Sci. Technol. **20**, 035018 (2011).
[16] R. Zhang, R.-J. Zhan, X.-H. Wen, and L. Wang, Plasma Sources Sci. Technol. **12**, 590 (2003).
[17] J. S. Eom and S. H. Kim, Thin Solid Film **516**, 4530 (2008).
[18] C.-Y. Lee, J.-H. Lee, D.-H. Choi, H.-J. Lee, H.-S. Kim, S.-B. Jung, and W.-C. Moon, Microelectron. Eng. **84**, 2653 (2007).
[19] B.-I. Noh, J.-W. Yoon, and S.-B. Jung, Int. J. Adhes. Adhes. **30**, 30 (2010).
[20] S. K. Rutledge and J. A. Mihelcic, Surface Coat. Technol. **39/40**, 607 (1989).
[21] N. Gherardi, G. Gouda, E. Gat, A. Ricard, and F. Massines, Plasma Source Sci. Technol. **9**, 340 (2000).
[22] Yu. B. Golubovskii, V. A. Maiorov, J. Behnke, and J. F. Behnke, J. Phys. D: Appl. Phys. **35**, 751 (2002).
[23] V. R. Soloviev and V. Kristov, J. Phys: Conf. Series. **927**, 012059 (2017).